JOURNAL OF SOLID STATE CHEMISTRY 36, 195–204 (1981)

Crystal Structure and Pyroelectric Coefficient of $Co(IO_3)_2$ and Structural Relationships among the Anhydrous Noncentrosymmetric 3*d*-Transition Metal Iodates

C. SVENSSON,* S. C. ABRAHAMS, AND J. L. BERNSTEIN

Bell Laboratories, Murray Hill, New Jersey 07974

Received April 3, 1980; in final form June 16, 1980

Cobalt iodate, $Co(IO_3)_2$, is pyroelectric at room temperature and crystallizes in the trigonal space group $P3$ with four formulas in the unit cell. The pyroelectric coefficient $p_3 = 5.1(5) \times 10^{-5}$ Cm^{-2} K^{-1}, and the lattice constants at 298 K are $a = 10.9597(1)$ and $c = 5.0774(1)$ Å. The crystal structure was solved from the Patterson function and a consideration of the structural similarities among the anhydrous 3*d*-transition metal iodates. Refinement was by the method of least squares using 1825 observed reflections measured with a four-circle diffractometer. The final agreement factor $R = 0.050$. Two of the three independent octahedrally coordinated cobalt atoms are disordered. The absolute orientation of the polar axis was determined with respect to the crystal morphology. The iodine atoms in the trigonal pyramidal iodate ions point toward the morphologically undeveloped end of the crystals, as does the positive sense of the spontaneous polarization: It is this end that develops a positive polarization on heating. The spontaneous polarization is estimated at about 22×10^{-2} Cm^{-2}. The iodate ion arrangement is very similar to that in α-$LiIO_3$. The anhydrous noncentrosymmetric 3*d*-iodates may be classified into three isomorphous sets, with space group $P6_3$ and corresponding maximal subgroups $P3$ and $P2_1$. All three sets are isostructural with α-$LiIO_3$ except for the cation distribution. The ability of the iodate ion framework to accept a range of cations of different valences is discussed in terms of the tricapped trigonal-prismatic environment about the iodine atoms.

1. Introduction

The transition metal iodates form a series of compounds with potentially useful dielectric and nonlinear optical properties. Most of the crystalline anhydrous iodates of the 3*d*-transition metals have been found to be noncentrosymmetric with a wide range in efficiency for generating second harmonics (*1–4*). The unit cell and symmetry of $Co(IO_3)_2$ was found (*1*) to resemble closely that of $Fe(IO_3)_3$, despite the difference in valency of the two 3*d*-elements. In addition, both iodates generate second harmonics at 1.06 μm with an efficiency about two orders of magnitude greater than powdered quartz. $Co(IO_3)_2$ remains paramagnetic to 1.4 K, whereas $Fe(IO_3)_3$ orders antiferromagnetically at $\Theta_N = 17$ K (*1*). The crystal structure of $Fe(IO_3)_3$ was recently reported (*4*). This paper presents the crystal structure of $Co(IO_3)_2$, the absolute determination of the pyroelectric coefficient p_3, and a rationalization of the structural chemistry of the anhydrous noncentrosymmetric 3*d*-transition metal iodates.

---

* Work performed while on leave from Inorganic Chemistry 2, Chemical Center, University of Lund, P.O. Box 740, S-220 07 Lund, Sweden.

0022-4596/81/020195-10$02.00/0

2. Experimental

A small crystal with dimensions 0 · 101 × 0 · 170 × 0 · 244 mm was cut from the morphologically undeveloped end of a pencil-shaped crystal (see Fig. 1) grown from boiling aqueous solution (*5*). The purple crystal was examined under the polarizing microscope for evidence of twinning or multiple domains: None were detected. The crystal was mounted on a Pyrex capillary. Slightly less than two-thirds of reciprocal space with radius $(\sin\theta)/\lambda \leq 0.8$ Å^{-1} was measured on an Enraf-Nonius CAD-4 diffractometer controlled by PDP 11/40-8e computer under Enraf-Nonius software (*6*). The radiation used was graphite monochromatised Mo$K\alpha$. An ω-2θ scan over an angular range of 1.3° + 0.3°tan θ with maximum scan time of 90s resulted in a counting statistical precision not less than 2%. Three standard reflections measured hourly decreased linearly during most of the measurements but irregularly although in parallel while measuring about 400 reflections toward the end of the experiment. The decrease was caused by a faulty monochromator assembly. At the end of the measurements the standard intensities had fallen to 42% of their initial values. The decline was fitted by a combination of linear equations and one third-order polynomial for the group of 400 reflections, giving a continuous correction curve. The internal agreement factor for the entire data set, based on averaged equivalent reflections, was 0.037: for 100 pairs of equivalent reflections with one member near the beginning and the other near the end of the experiment, the internal agreement factor was 0.041. Corrections were also made for Lorentz, polarization and absorption effects. Transmission factors ranged from 0.09 to 0.30.

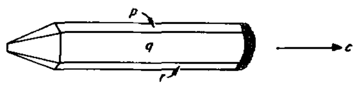

FIG. 1. Morphology of Co(IO$_3$)$_2$ crystal: $p(\bar{2}1.0)$, $q(11.0)$, $r(\bar{1}2.0)$, with sense of trigonal c-axis shown.

A total 5378 structure factors were measured, resulting in 3033 *Fmeas* after averaging equivalent reflections in point group 3. Standard deviations were derived from the expression $\sigma^2F^2meas = f\{V_1 + V_2\}$(*7*), with $V_1 = 29 \times 10^{-4}\ (Fmeas)^4$ and $V_2 = 80 \times 10^{-4}\ (Fmeas)^4$. On the basis that reflections with $|Fmeas|^2 < 4\sigma|Fmeas|^2$ are regarded as unobserved, 1208 terms were omitted from further analysis. The minimum value of $\sigma Fmeas$ for $|Fmeas| < 180$ on the absolute scale was taken as 9.1. The magnitudes of the remaining 1825 symmetry-independent *Fmeas* and $\sigma Fmeas$ on the final least-squares derived absolute scale are given in Ref. *8*.

3. Crystal Data

Co(IO$_3$)$_2$ has formula weight 408.74. The trigonal unit cell has lattice constants $a = 10.9597(1)$ and $c = 5.0774(1)$ Å at 298 K, obtained by the method of least squares from the spacings of diffraction lines measured on a film exposed in an IRDAB Guinier-Hägg camera, using Cu$K\alpha_1$ = 1 · 540598 Å with Al$_2$O$_3$ ($a = 4.75890$, $c = 12.99105$ Å) as internal standard. The unit cell volume is 528.16 Å^3. $Dx = 5.140$ g cm^{-3} for four formula weights per unit cell. The Laue symmetry is pseudohexagonal. Space groups $P6_3$ or $P6_322$ were originally assigned (*1*) on the basis of the systematic absence of $00l$ for $l = 2n + 1$. The alternative centrosymmetric space groups are eliminated by the observation that second harmonics are generated in the powder (*1*). The full structure determination shows the symmetry to be trigonal, with space group $P3$. Further crystal data are given in Refs. *1* and *9*.

4. Solution and Refinement of the Structure

Striking similarities exist among the structures of hexagonal α-$LiIO_3$ (*10, 11*), hexagonal $Fe(IO_3)_3$ (*4*), and monoclinic α-$Cu(IO_3)_2$ (*3*) (see Section 10). A consideration of these structural similarities, the metric relationships among the unit cell constants given in Table I, and solution of the three-dimensional Patterson function, led to the construction of structural models for $Co(IO_3)_2$ in space group $P6_3$ and in maximal subgroups $P3$ and $P2_1$. Different arrangements of the Co^{2+} ions relative to the IO_3^- ion framework were tested, but only the model in space group $P3$ with partially disordered Co^{2+} ions refined acceptably. Atomic scattering factors and anomalous dispersion corrections were taken from the *International Tables for X-Ray Crystallography* (*12*). The model was refined by the method of least squares, initially on the PDP 11/40 computer using Enraf-Nonius software (*13*) and finally on the Honeywell 6080 computer with ORFLS (*14*). In the initial refinements, all shifts in the last cycle of iterations were less than 0.1 of the associated estimated standard deviation (e.s.d.) and gave $R = 0.0496$, $wR = 0.0697$, and $S = 0.887$ (7). In the final refinements, no shift was larger than 0.02 e.s.d., with corresponding $R = 0.0502$, $wR = 0.0697$, and $S = 0.889$, values essentially unchanged from the initial indicators: including the unobserved reflections, $R = 0.0690$. However, differences as large as 1.8 e.s.d. were noted between the two sets of position coordinates, particularly among the z-coordinates: the final e.s.d.'s were also found to be larger, some by as much as a factor of 2. Inadequate refinement has also been noted in space group $P6_5$ with Enraf-Nonius software (*13*). Final values of the refined atomic position coordinates are given in Table II, anisotropic thermal parameters in Table III.

5. Absolute Configuration and Polar Axis Orientation

Assignment of a right-handed set of crystallographic axes to the crystal used for measuring the integrated intensities gave the direction of the undeveloped end of the pencil shaped crystal as parallel to the c-axis (see Fig. 1). The absolute atomic arrangement in this polar crystal may be determined from the Bijvoet differences arising from anomalous scattering of Mo$K\alpha$ radiation by the Co, I, and O atoms, which result in $|F(hk\cdot l)| \neq |F(h+k, \bar{h}\cdot\bar{l})|$ (*8*). The hypothesis that the anisotropic thermal vibration model with $\bar{x}\bar{y}\bar{z}$ coordinates fits the structure factors listed in Ref. *8* better than that with xyz coordinates is readily tested, since $wR(\bar{x}\bar{y}\bar{z}) = 0.0708$, $wR(xyz) = 0.0697$. The theoretical value of $wR(\bar{x}\bar{y}\bar{z})/wR(xyz)$

TABLE I

UNIT CELL DIMENSIONS OF RELATED IODATES

Iodate	Space Group	Unit cell dimensions	Reference
α-$LiIO_3$	$P6_3$	$a = 5.481$ Å, $c = 5.171$ Å	*10, 11*
$Fe(IO_3)_3$	$P6_3$	$a = 9.225$, $c = 5.224$	*4*
$Co(IO_3)_2$	$P3$	$a = 10.9597$, $c = 5.0774$	This work
α-$Cu(IO_3)_2$[a]	$P2_1$	$a = 5.569$, $c = 5.111$, $b = 9.270$ Å $\gamma = 95.82°$	*2, 3*

[a] With c-axis taken as unique (i.e., first setting).

TABLE II

FINAL ATOMIC POSITION COORDINATES OF $Co(IO_3)_2$ AT 298 K[a]

Atom	x	y	z
Co(1)	0	0	0.5716(9)
Co(2)	0.5057(3)	0.9967(3)	0.0758(9)
Co(3)	0.5019(7)	0.9971(7)	0.5593(16)
I(1)	$\frac{2}{3}$	$\frac{1}{3}$	0
I(2)	$\frac{1}{3}$	$\frac{2}{3}$	0.48365(57)
I(3)	0.67633(13)	0.83187(15)	0.98658(48)
I(4)	0.82227(13)	0.65680(10)	0.49152(44)
O(1)	0.8266(11)	0.3769(13)	0.8235(32)
O(2)	0.4676(14)	0.8188(13)	0.3093(33)
O(3)	0.9506(10)	0.8213(9)	0.3421(24)
O(4)	0.8602(15)	0.5399(13)	0.2969(29)
O(5)	0.6718(13)	0.6317(14)	0.3027(30)
O(6)	0.6396(14)	0.9579(14)	0.8259(31)
O(7)	0.8243(10)	0.8570(11)	0.7950(23)
O(8)	0.5425(11)	0.6743(11)	0.8338(27)

[a] All atoms are in threefold positions except for Co(1), I(1), and I(2) which are in onefold positions. Atoms Co(2) and Co(3) are nominally in threefold positions but are occupied by only 2.021(42) and 1.094(46) atoms, respectively.

at the half-percent significance level for 1825 independent *Fmeas* and 119 variables is $R_{1,1704,0.005} = 1.0023$ (*15*): the experimental value is 1.0158, hence the hypothesis may be rejected. The coordinates of Table II hence represent the absolute atomic configuration of $Co(IO_3)_2$ in terms of the Miller indices and structure factor magnitudes in Ref. *8*, i.e., the iodine atom in each IO_3^- trigonal pyramidal ion is directed parallel to the *c*-axis, or toward the undeveloped end of the pencil-shaped crystal as depicted in Fig. 1.

6. Arrangement of Co^{2+} Ions in $Co(IO_3)_2$

Each general location in space group *P*3 has three equivalent positions in the unit cell: only two of these three positions are occupied by Co(2) and only one of them by Co(3) in the final structural model for $Co(IO_3)_2$ as given in Table II. Full occupancy of the two locations would result in repeated Co(2)–Co(3) contacts along the *c*-axis of about $c/2$ or 2.54 Å. The model implies that, on average, each Co^{2+} ion has only two close Co^{2+} neighbors at the same *z*-level about 5.5 Å distant. Complete cat-

TABLE III

ANISOTROPIC THERMAL PARAMETERS OF $Co(IO_3)_2$ AT 298 K[a]

Atom	β_{11}	β_{22}	β_{33}	β_{12}	β_{13}	β_{23}
Co(1)	23(2)	23	83(11)	12	0	0
Co(2)	31(3)	28(3)	89(12)	22(2)	−10(4)	9(4)
Co(3)	26(6)	36(6)	181(27)	10(5)	−19(8)	1(9)
I(1)	458(14)	458	1093(69)	229	0	0
I(2)	524(17)	524	433(59)	262	0	0
I(3)	167(10)	547(14)	971(36)	127(11)	58(14)	−93(17)
I(4)	459(13)	77(8)	368(29)	46(9)	62(16)	−37(13)
O(1)	12(8)	38(11)	303(60)	8(8)	12(17)	34(19)
O(2)	48(12)	25(10)	295(61)	15(9)	−40(21)	5(18)
O(3)	37(9)	3(7)	173(40)	8(7)	46(15)	14(13)
O(4)	62(13)	34(10)	193(46)	30(10)	23(19)	−17(17)
O(5)	23(10)	43(12)	212(51)	−3(8)	10(17)	−38(19)
O(6)	48(12)	50(13)	264(55)	38(10)	17(20)	−37(21)
O(7)	15(8)	28(8)	107(34)	10(7)	19(12)	5(13)
O(8)	13(8)	16(9)	224(47)	−19(15)	−19(15)	19(16)

[a] The form of the temperature factor is exponential $-(\beta_{11}h^2 + \beta_{22}k^2 + \beta_{33}l^2 + 2\beta_{12}hk + 2\beta_{13}hl + 2\beta_{23}kl)$. The coefficients for Co and O are $\times 10^4$, for I $\times$ 10^5. Note that atom O(8) is, insignificantly, nonpositive definite.

ion ordering of this kind is found in the limiting case of α-$Cu(IO_3)_2$ (*3*).

The possibility that the symmetry of $Co(IO_3)_2$ is lower than trigonal was investigated, although it was apparent that any such departure would be small. A likely candidate, in view of the structural similarities with α-$Cu(IO_3)_2$, was the space group $P2_1$. The original measured structure factors were thereupon reindexed and reaveraged in terms of monoclinic symmetry to give 3447 independent *Fmeas*. Three models were refined, by the method of least squares, differing in the choice of origin. All gave final values of R about 0.14, the lowest being 0.135. The monoclinic model was hence rejected. There is also a possibility that the symmetry is lower than trigonal but with the crystal twinned such that trigonal symmetry is mimicked. High-angle reflections from the crystal studied showed no indications of twinning, although other crystals of $Co(IO_3)_2$ are clearly twinned by small relative rotations about the *c*-axis.

Inspection of the interatomic distances in Table IV, corresponding to the atomic coordinates in Table II, shows that Co(1)–O has the normal distance (*30*) of about 2.10 Å for high-spin Co^{2+}. The distances for Co(2)–O are as much as 0.06 Å longer, and those for Co(3)–O range up to 0.13 Å longer. These ranges could be due to an incorrect choice of space group, but may also be expected as a consequence of the disordered $Co(2)^{2+}$ and $Co(3)^{2+}$ ions. The oxygen atoms forming the vacant octahedral interstices are likely to be slightly further apart than in occupied octahedra and the positions given in Table I must average both sets. The temperature factors for O(3) and O(7) which are octahedrally bonded only to Co(1) are indeed smaller than

TABLE IV

INTERATOMIC DISTANCES (IN Å) AND ANGLES (IN DEGREES)

Co(1)–O(3)	2.10(1)	(3×)	I(1)–O(1)	1.81(1) Å	(3×)
O(7)	2.11(1)	(3×)	O(4)	2.66(1)	(3×)
Co(2)–O(4)	2.09(1)		I(2)–O(2)	1.80(1)	(3×)
O(5)	2.13(1)		O(8)	2.87(1)	(3×)
O(6)	2.14(1)				
O(2)	2.15(1)				
O(8)	2.15(1)		I(3)–O(8)	1.79(1)	
O(1)	2.16(1)		O(7)	1.79(1)	
			O(6)	1.81(1)	
			O(5)	2.70(2)	
Co(3)–O(5)	2.18(2)		O(2)	2.76(2)	
O(1)	2.19(2)		O(3)	2.90(1)	
O(2)	2.21(2)				
O(8)	2.22(2)		I(4)–O(3)	1.81(1)	
O(6)	2.22(2)		O(5)	1.81(1)	
O(4)	2.23(2)		O(4)	1.82(1)	
			O(7)	2.67(1)	
			O(1)	2.79(1)	
			O(6)	2.85(2)	
O(1)–I(1)–O(1)	97.5(6)	(3×)			
O(2)–I(2)–O(2)	98.0(6)	(3×)	O(4)–I(4)–O(5)	96.7(6)	
O(6)–I(3)–O(8)	98.8(6)		O(3)–I(4)–O(5)	97.2(6)	
O(7)–I(3)–O(8)	98.9(6)		O(3)–I(4)–O(4)	97.8(5)	
O(6)–I(3)–O(7)	99.6(6)				

those for the remaining oxygen atoms bonded to Co(2) and Co(3) (see Table III): The average radial RMS amplitude of vibration of these atoms is 0.143 Å, that of O(3) and O(7) is 0.100 Å.

7. Iodate Ion Dimensions in $Co(IO_3)_2$

The dimensions of the four independent iodate ions in $Co(IO_3)_2$, as listed in Table IV, compare closely with the values reported in recent determinations of other iodates. Each iodine atom is linked to three oxygen atoms at an average distance of 1.805 Å with average O–I–O angle of 98.0° in $Co(IO_3)_2$. In each ion, the iodine is also linked through the lone electron pair to three additional oxygen atoms at an average distance of 2.772 Å. The I–O bond length averaged over 45 independent I–O bonds measured in the present series of investigations on transition metal iodates is 1.808 Å. The lone pair contacts, as expected, are more variable in length and range from 2.6 to 3.2 Å.

8. Spontaneous Polarization in $Co(IO_3)_2$

$Co(IO_3)_2$ is pyroelectric and hence develops an electric polarization under a change of temperature: the space group permits only the pyroelectric coefficient p_3 to be nonzero. The polarization change, for zero thermal expansion, is due to the relative displacement of the Co^{2+} and IO_3^- ions together with possible rotations of the dipoles associated with the IO_3^- ions and electronic redistribution as a function of temperature (*16*). It is possible to estimate the magnitude and sense of the spontaneous polarization in $Co(IO_3)_2$ from the atomic positions given in Table II, although an experimental value cannot be measured since the crystal is not ferroelectric. Several assumptions are made to simplify the calculation: the negative point charge associated with the IO_3^- ion is taken at the electron density centroid, and a mean value of z is taken for ions of like sign with similar z-coordinates. Thus, there are four positive point charges per unit cell at $z = 0.0753$ and 0.5660, four negative point charges per unit cell at $z = 0.9362$ and 0.4344. The resulting polarization is hence about 16.7×10^{-2} Cm^{-2}, with positive sense parallel to the c-axis. In addition, the dipole contribution of the eight IO_3^- ions, assuming about 1D(3.3×10^{-30} C · m) per ion, totals about 5×10^{-2} Cm^{-2} in the same sense as the point charge contribution, for a total of about 21.7×10^{-2} Cm^{-2}.

The calculated spontaneous polarization in $Co(IO_3)_2$ is somewhat larger than in α-$LiIO_3$ (*17*), but with similar sense (*18*) as given by the vector from the triangular oxygen face of the iodate ion toward the iodine atom. In $Co(IO_3)_2$, P_s is directed toward the rounded end of the crystal (see Fig. 1) whereas in $LiIO_3$ it is directed toward the smaller end (*18*).

9. Absolute Sense and Value of the Pyroelectric Coefficient in $Co(IO_3)_2$

An approximate value for the p_3 pyroelectric coefficient was obtained from a small single crystal with cross-section of 0.30 × 0.18 mm. Silver paste electrodes were applied to both ends (cf. Fig. 1), and the polarization change produced on heating the crystal slowly from room temperature through intervals ranging from 30 to 60° measured with a Keithley 610C electrometer. The resulting value for p_3, which is the sum of both the primary and secondary pyroelectric coefficients, was $5.1(5) \times 10^{-5}$ Cm^{-2} K^{-1}. The rounded end of the crystal developed a positive polarization on heating, hence $p_3 > 0$ (see Section 5). Since the spontaneous polarization is directed toward the same end of the crystal, it may be inferred that P_s increases with increasing temperature, as is also the case for α-$LiIO_3$, α-$Cu(IO_3)_2$, and $Nd(IO_3)_3 \cdot H_2O$ (*17*).

10. Structural Relationships among the Anhydrous Noncentrosymmetric 3*d*-Transition Metal Iodates

Several anhydrous iodates of the 3*d*-transition elements have been prepared and characterized (*1, 2, 9, 19*), including two crystalline forms of $Sc(IO_3)_3$, one each of $Mn(IO_3)_2$, $Fe(IO_3)_3$, and $Co(IO_3)_2$, two of $Ni(IO_3)_2$, and three of $Cu(IO_3)_2$. One of the scandium iodates and two copper iodates are centrosymmetric, the remainder lack inversion centers. X-Ray powder data have been published for all 10 compounds (*1, 2, 19*) and most of the patterns have been indexed. The crystal structure of α-$Cu(IO_3)_2$ has been determined (*3*), also that of hexagonal $Fe(IO_3)_3$ (*4*). The length of the *a*-axis in the unit cell of $Fe(IO_3)_3$ (*4*) is related to that given in the powder assignment (*1*) by $\sqrt{3}/2$, i.e., corresponding to a rotation of 30° about the hexagonal axis. The powder pattern of β-$Sc(IO_3)_3$ and $Cr(IO_3)_3$ could also be indexed using lattice constants comparable to those of $Fe(IO_3)_3$ (*4*). The powder data (*2*) for α-$Ni(IO_3)_2$ can be fitted to a unit cell similar to that of α-$Cu(IO_3)_2$, assuming that the sample contains some β-$Ni(IO_3)_2$ as a second phase and omitting some diffuse lines (see Table V).

The anhydrous noncentrosymmetric 3*d*-transition metal iodates may hence be divided into three groups:

Space group:	$P6_3$	$P3$	$P2_1$
3*d*-iodate:	$Fe(IO_3)_3$ $Cr(IO_3)_3$ β-$Sc(IO_3)_3$	$Co(IO_3)_2$ $Mn(IO_3)_2$ β-$Ni(IO_3)_2$	α-$Cu(IO_3)_2$ α-$Ni(IO_3)_2$

The structures of these eight iodates are sufficiently similar that definitive assignment of space group to each crystal must probably await their complete structural determination. Although there are two different stoichiometries, with different unit cells and space groups, all are closely related to the parent structure of α-$LiIO_3$.

The idealized structure of α-$LiIO_3$ together with that of the 3*d*-iodates is shown in Fig. 2, the four basic unit cells also being indicated. The framework of iodate ions remains essentially unchanged throughout the series of compounds, only the occupancy of the face-sharing octahedral interstices differing. The occupied octahedra become increasingly distorted on passing from the atomic arrangement in α-$LiIO_3$ through that of $Co(IO_3)_2$ and $Fe(IO_3)_3$ to the structure of α-$Cu(IO_3)_2$. As expected, the Cu environment is tetragonally distorted. The large increase in monoclinic angle from the 95.1° of α-$Cu(IO_3)_2$ (*2*) to that proposed for α-$Ni(IO_3)_2$ (see Table V) could be the result of even larger distortion about Ni^{2+} due to a tendency toward square planar coordination. The exothermic transforma-

TABLE V

POWDER PATTERN OF α-$Ni(IO_3)_2$[a]

hkl	d_{obs} (Å)	d_{calc} (Å)	I_{obs}
$\bar{1}10$	5.06	5.10	3
011	4.43	4.41	1
101	3.72	3.73	8
$\bar{1}11$	3.63	3.61	10
111	3.29	3.28	7
120	3.13	3.13	1
121	2.67	2.67	10
130	2.39	2.39	3
102	2.31	2.31	5

[a] Based on a unit cell similar to that of α-$Cu(IO_3)_2$ with $a = 5.67(4)$, $b = 8.95(7)$, $c = 5.10(2)$ Å, and $\gamma = 101.3(5)°$. For two formula units per cell, the calculated density is 5.34 g cm^{-3}.

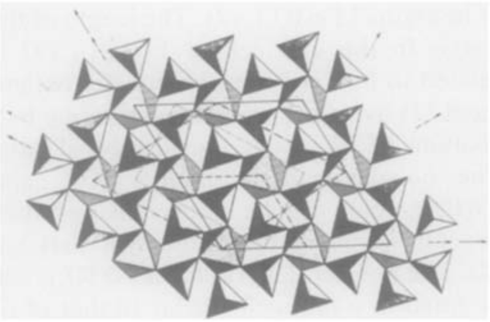

FIG. 2. Idealized structure and relationships among the unit cells of α-$LiIO_3$, $Co(IO_3)_2$, $Fe(IO_3)_3$, and α-$Cu(IO_3)_2$ as projected along the *c*-axes. The atomic coordinates in the figure are transformed from the published values of α-$LiIO_3$ (*10*) by the matrix (010/100/00$\bar{1}$), from those of $Co(IO_3)_2$ in this paper by (010/100/001) and from those of α-$Cu(IO_3)_2$ (*3*) by (100/001/0$\bar{1}$0). No transformation was made for $Fe(IO_3)_3$ (*4*). Solid outline represents $Co(IO_3)_2$, dashed α-$LiIO_3$, dotted α-$Cu(IO_3)_2$, and dot-dashed $Fe(IO_3)_3$ unit cell.

tion of α- to β-$Ni(IO_3)_2$ occurring about 775K (*9*), just below the decomposition temperature, may hence be a displacive phase transition involving a rearrangement toward a more regular octahedral Ni-coordination.

TABLE VI

IODATE ION AND UNIT CELL VOLUMES OF THE 3*d*-TRANSITION METAL IODATES OF THE α-$LiIO_3$ TYPE[a]

Compound	Number of formula units per cell	Unit cell volume (Å^3)	IO_3^- ion volume (Å^3)
α-$LiIO_3$	2	134.5	67.2
$Co(IO_3)_2$	4	528.2	66.0
$Mn(IO_3)_2$	4	544.7	68.1
β-$Ni(IO_3)_2$	4	518.3	64.8
$Fe(IO_3)_3$	2	385.0	64.2
$Cr(IO_3)_3$	2	373.1	62.2
β-$Sc(IO_3)_3$	2	403.6	67.3
α-$Cu(IO_3)_2$	2	262.5	63.4
α-$Ni(IO_3)_2$	2	253.8	63.4

[a] For comparison, the volume of each IO_3^- ion in HIO_3 is 62.4 Å^3: the structure of HIO_3 is different from the iodates in Table VI.

The general iodate ion framework shown in Fig. 2 is able both to accommodate various metal ions with radii in the range 0.8–0.9 Å and also allow for different arrangements of the metal ions to compensate for changes in valency. Thus every third column of octahedra along the hexagonal axis in $Fe(IO_3)_3$ is completely unoccupied, and these octahedra are least distorted. An indication of the stability of the iodate ion framework is

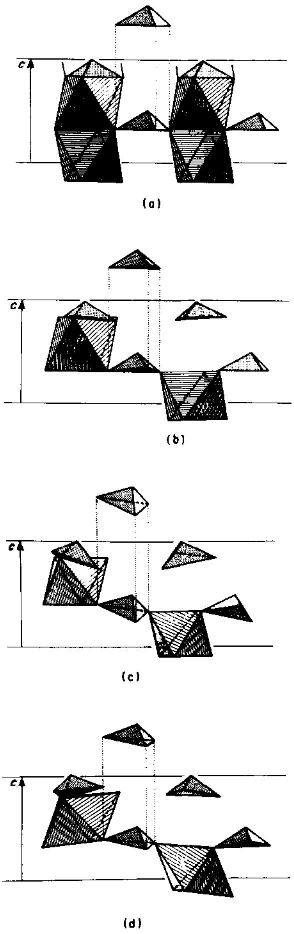

FIG. 3. Projections of the idealized structures of (a) α-$LiIO_3$, (b) $Co(IO_3)_2$, (c) $Fe(IO_3)_3$, and (d) α-$Cu(IO_3)_2$ on a plane perpendicular to that shown in Fig. 2. The tricapped trigonal prism of oxygen atoms around the iodine atom in each structure is indicated by dotted lines. Only in (b) are all crystallographically independent iodate and MO_6 octahedra not included.

given by the formation of solid solutions of HIO_3 in α-$LiIO_3$ (*20–22*). As much as one-third of the lithium in this structure can be exchanged for hydrogen with only small changes in the dimensions of the unit cell that vary linearly with hydrogen substitution (*20*).

The effective volume of an IO_3^- ion in this group of iodates varies by less than 10%, as shown in Table VI. The packing density of the iodate ion decreases as the cation radius increases and as the number of occupied octahedra increases. In $Li_{1-x}H_xIO_3$, the volume per IO_3^- ion decreases from 67.2 to 66.2 Å^3 as x increases from 0 to 0.35 (*20*). On the assumption that the iodine atom with its lone pair of electrons occupies the same volume as each oxygen atom (*23, 24*), the volume per oxygen atom in these iodates is about 16.5 Å^3, in good agreement with the normal range of 15 to 17 Å^3 in simple close-packed oxides. The iodine atom lone pair points toward the center of a tricapped trigonal prism in each of the four basic structures shown in Fig. 2, as illustrated in Fig. 3. In the most regular structure of the group, that of α-$LiIO_3$, the distance from the iodine atom to the center of the prism (see Fig. 3a) is 1.70 Å, where the expected distance (*24*) is 1.25 Å. The distances from the center of the prism to the oxygen atoms are 3.15 Å (3×) and 3.17 Å (6×).

The structure of $Y(OH)_3$, with similar oxygen packing but with Y^{3+} at the centers of the trigonal prisms (*25*), is strikingly similar to that of α-$LiIO_3$ from this viewpoint. The YO_9 prism is smaller, with Y–O about 2.50 Å: The unoccupied octahedral interstices are accordingly compressed along c and expanded normal to this direction. The detailed distortion from hexagonal close-packing found in α-$LiIO_3$ (see Fig. 4) is possibly caused by the tendency to assume the energetically more favorable tricapped trigonal prismatic environment. This possibility is supported by the appearance of similar tricapped trigonal prisms in other iodates, e.g., in HIO_3 (*26, 27*), $CuIO_3(OH)$ (*28*), and $Cu(IO_3)_2 \cdot 2H_2O$ (*28*). A similar coordination is also found about the As atom with its lone pair of electrons in $AsCl_3$ (*29*). It is the rather large prisms associated with iodine in the α-$LiIO_3$ structure that provides the adjustability in structure discussed above.

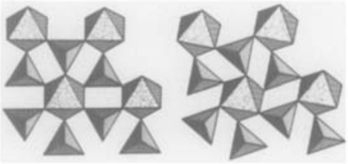

FIG. 4. (Left) Hexagonal close packing in α-$LiIO_3$ type structure if iodate groups were regular tetrahedra; (right) distorted hexagonal close packing, in α-$LiIO_3$.

Acknowledgments

It is a pleasure to thank K. Nassau for growing the crystals used: One of us (C.S.) also wishes to thank the Swedish Natural Sciences Research Council, the Swedish National Board for Technical Development, and the Fulbright exchange program for grants.

References

1. S. C. ABRAHAMS, R. C. SHERWOOD, J. L. BERNSTEIN, AND K. NASSAU, *J. Solid State Chem.* **7**, 205 (1973).
2. S. C. ABRAHAMS, R. C. SHERWOOD, J. L. BERNSTEIN, AND K. NASSAU, *J. Solid State Chem.* **8**, 274 (1973).
3. R. LIMINGA, S. C. ABRAHAMS, AND J. L. BERNSTEIN, *J. Chem. Phys.* **62**, 4388 (1975).
4. M. JANSEN, *J. Solid State Chem.* **17**, 1 (1976).
5. K. NASSAU, *J. Crystal Growth* **15**, 171 (1972).
6. "Enraf-Nonius CAD-4 Operation Manual" (Delft, unpublished) 1979.
7. S. C. ABRAHAMS, J. L. BERNSTEIN, AND E. T. KEVE, *J. Appl. Crystallogr.* **4**, 284 (1971).
8. See NAPS document No. 3708 for 8 pages of supplementary material. Order from ASIS/NAPS c/o Microfiche Publications, P.O. Box 3513, Grand Central Station, New York, New York, 10163. Remit in advance for each NAPS Accession number. Institutions and organizations may use purchase orders when ordering; however,

there is a billing charge for this service. Make checks payable to Microfiche Publications. Photocopies are $5.00. Microfiche are $3.00. Outside the U.S. and Canada, postage is $3.00 for a photocopy or $1.50 for a fiche.

9. K. Nassau, J. W. Shiever, and B. E. Prescott, *J. Solid State Chem.* **7**, 186 (1973).
10. A. Rosenzweig and B. Morosin, *Acta Crystallogr.* **20**, 758 (1966).
11. J. L. de Boer, F. van Bolhuis, F. Olthof-Hazekamp, and A. Vos, *Acta Crystallogr.* **21**, 841 (1966).
12. "International Tables for X-ray Crystallography" (J. A. Ibers and W. C. Hamilton, Eds.), Vol. IV. Kynoch, Birmingham (1974).
13. "Enraf-Nonius Structure Determination Package" (B. Frenz, Ed.). Molecular Structure Corporation, College Station (1979).
14. W. R. Busing, K. O. Martin, and H. A. Levy, *J. Appl. Crystallogr.* **6**, 309 (1973).
15. W. C. Hamilton, *Acta Crystallogr.* **18**, 502 (1965).
16. S. C. Abrahams, *Mat. Res. Bull.* **13**, 1253 (1978).
17. R. Liminga and S. C. Abrahams, *J. Appl. Crystallogr.* **9**, 42 (1976).
18. E. H. Turner, *J. Appl. Crystallogr.* **9**, 52 (1976).
19. K. Nassau and J. W. Shiever, *J. Solid State Chem.* **13**, 368 (1975).
20. S. A. Hamid, G. Kunze, and G. Reuter, *Acta Crystallogr. Sect. A* **33**, 261 (1977).
21. S. A. Hamid and G. Kunze, *Acta Crystallogr. Sect. A* **33**, 264 (1977).
22. S. A. Hamid, *Phys. Stat. Solidi, Sect. A* **43**, K29 (1977).
23. S. Andersson and A. Åström, Nat. Bur. Stand. (US), Spec. Publ., Proc. Fifth Mat. Symp., p. 3 (1972).
24. J. Galy, G. Meunier, S. Andersson, and A. Åström, *J. Solid State Chem.* **13**, 142 (1975).
25. K. Schubert and A. Seitz, *Z. Naturforsch.* **1**, 324 (1946).
26. M. T. Rogers and L. Helmholz, *J. Amer. Chem. Soc.* **63**, 278 (1941).
27. S. Andersson, *Acta Crystallogr. Sect. B* **35**, 1321 (1979).
28. S. Ghose and C. Whan, *Amer. Min.* **63**, 172 (1978).
29. R. Enjalbert and J. Galy, *C.R. Acad. Sci. Paris, Sect. C* **278**, 259 (1978).
30. R. D. Shannon, *Acta Crystallogr. Sect. A* **32**, 751 (1976).